Safe CO2 threshold limits for indoor long-range airborne transmission control of COVID-19

Article

Accepted Version

It is advisable to refer to the publisher's version if you intend to cite from the work. See [Guidance on citing](#).

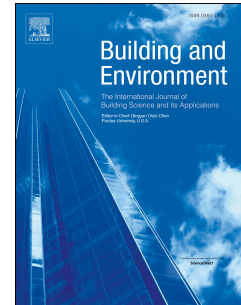# www.reading.ac.uk/centaur

CentAUR

Central Archive at the University of Reading

Reading's research outputs online

Journal Pre-proof

Safe CO$_2$ threshold limits for indoor long-range airborne transmission control of COVID-19

Xiaowei Lyu, Zhiwen Luo, Li Shao, Hazim Awbi, Samuele Lo Piano

Please cite this article as: Lyu X, Luo Z, Shao L, Awbi H, Lo Piano S, Safe CO$_2$ threshold limits for indoor long-range airborne transmission control of COVID-19, *Building and Environment* (2023), doi: https://doi.org/10.1016/j.buildenv.2022.109967.

This is a PDF file of an article that has undergone enhancements after acceptance, such as the addition of a cover page and metadata, and formatting for readability, but it is not yet the definitive version of record. This version will undergo additional copyediting, typesetting and review before it is published in its final form, but we are providing this version to give early visibility of the article. Please note that, during the production process, errors may be discovered which could affect the content, and all legal disclaimers that apply to the journal pertain.

1 Manuscript revised to Building and Environment, Dec 2022

2

Safe CO₂ Threshold Limits for Indoor Long-range Airborne Transmission

3

Control of COVID-19

4

5 Xiaowei Lyu[1], Zhiwen Luo[2]*, Li Shao[1], Hazim Awbi[1], Samuele Lo Piano[1]

6 1. School of the Built Environment, University of Reading, UK

7 2. Welsh School of Architecture, Cardiff University, UK

8 Correspondence: Prof Zhiwen Luo (LuoZ18@Cardiff.ac.uk)

9 **Abstract**: CO_2-based infection risk monitoring is highly recommended under the current

10 COVID-19 pandemic. However, the CO_2 monitoring thresholds proposed in the literature are

11 mainly for spaces with fixed occupants. Determining CO_2 threshold is challenging in spaces

12 with changing occupancy due to the co-existence of quanta and CO_2 remaining from the

13 previous occupants. Here, we propose a new calculation framework to derive safe excess CO_2

14 thresholds (above outdoor level), C_t, for various spaces with fixed/changing occupancy and

15 analyze the uncertainty entailed. Common indoor spaces were categorized into three scenarios

16 according to their occupancy condition, e.g., fixed or varying infection ratios

17 (infectors/occupants). We proved that rebreathed fraction-based model can be directly applied

18 for C_t derivation in the cases of a fixed infection ratio (Scenario 1 and Scenario 2). In the case

19 of varying infector ratios (Scenario 3), C_t derivation has to follow the general calculation

20 framework due to the existence of initial quanta/excess CO_2. Otherwise, significant bias can be

21   caused for C_t (e.g., 260 ppm) when infection ratio varies remarkably. C_t significantly varies

22   with specific space factors such as occupant number, activities, and community prevalence,

23   e.g., 7 ppm for gym and 890 ppm for lecture hall, indicating C_t should be determined on a case-

24   by-case basis. An uncertainty of C_t up to 6 orders of magnitude was found for all cases due to

25   uncertainty in emissions of quanta and CO_2, thus emphasizing the role of accurate emissions

26   data in obtaining C_t.

27

28   **Keywords:** infection risk control, CO_2 monitoring, initial quanta, uncertainty analysis

29

Nomenclature		
B	Breathing rate, m^3/h	
$C_{CO2,i}$	CO_2 concentration for occupancy stage i, ppm	
$C_{\text{Cin},i}$	Initial CO_2 concentration for occupancy stage i, ppm	
$C_{q,i}$	Quanta concentration for occupancy stage i, quanta/m^3	
$C_{qin,i}$	Initial quanta concentration for occupancy stage i, quanta/m^3	
C_t	Safe excess CO_2 threshold, ppm	
C_{t50}	Median safe excess CO_2 threshold, ppm	
E_{co2}	CO_2 emission rate, mL/s	
E_q	Quanta emission rate, quanta/h	
I_i	Infector number for occupancy stage i	
N_{ave}	Average occupant number	
N_i	Occupant number for occupancy stage i	
P_i	Infection risk for occupancy stage i	
P_t	Predefined infection risk threshold	
P_I	Community prevalence	
T_i	Exposure time for occupancy stage i, h	
V	Space volume, m^3	
λ_i	Air change rate for occupancy stage i, h^{-1}	

30

31   **1. Introduction**

32   COVID-19, as a novel coronavirus disease, has caused a worldwide pandemic spreading

33   since the end of 2019 (Chen et al., 2020). Indoor transmission control is the key to prevent the

34   spread of the SARs-CoV-2 virus due to a higher transmission risk indoors than outdoors (Qian

35   et al., 2020). The four main transmission routes in indoor environments are droplet-borne,

36   fomite, short-range airborne, and long-range airborne (Li, 2021; Wei and Li, 2016). Although

37   short-range airborne transmission route was inferred to be the dominant route in close contact

38   (Chen et al., 2020), long-range airborne transmission was revealed to more likely induce

39   outbreaks in poorly ventilated and confined indoor spaces (Peng et al., 2022). Thus, it is of

40   primary importance to monitor and control long-range airborne transmission for indoor

41   environment.

42   The exhaled infectious aerosols contributing to long-range airborne transmission are difficult

43   to detect, and can travel a long distance in indoor environment. Therefore, a detectable indicator

44   for transmission risk is urgently needed to effectively monitor long-range airborne transmission.

45   CO_2 that can be easily monitored through low-cost sensors (Peng and Jimenez, 2021) has been

46   recommended as risk indicator for long-range airborne transmission because it can both reflect

47   the indoor ventilation condition and the quanta concentration (Persily et al, 2022). Accordingly,

48   safe CO_2 thresholds are defined as the maximum CO_2 concentration level under which the

49   indoor space is at an acceptable infection risk. Such information is useful to guide the design

50   of infection-resilient buildings.

51   Treating CO_2 as an indicator for indoor ventilation performance, recent studies made use of

52   CO_2 thresholds for risk control based on prevailing ventilation standards with a target of

53   acceptable indoor air quality (IAQ) but not infection risk (CIBSE, 2021; SAGE-EMG, 2021;

54   REHVA, 2021). ASHRAE does not recommend a specific value of threshold (Persily et al.,

55   2022), although other organizations have suggested specific thresholds of 800 ppm (SAGE-

56   EMG, 2020; CDC, 2021) or 800-1000 ppm (REHVA, 2021) to ensure a safe indoor

57   environment. However, whether a fixed CO_2 threshold could guarantee a low infection risk

58   for all spaces is questionable considering factors such as occupancy level and respiratory

59   activity can all affect the value of it (Peng and Jimenez, 2021).

60   Moving beyond the assessment of CO_2 as a mere indicator of indoor ventilation condition,

61   CO_2 can also be used to directly reflect quanta concentration as CO_2 and virus-laden aerosols

62   can be co-produced and co-inhaled by human. Therefore, CO_2 thresholds can be calculated

63   backward by pre-defining an acceptable infection risk level (Hou et al., 2021; Peng and

64   Jimenez, 2021). Indoor airborne transmission risk can be maintained under the predefined risk

65   level in as much indoor CO_2 concentration can be maintained below the derived threshold.

66   Occupancy level and respiratory activity for a particular indoor space can all be factored in this

67   backward calculation process (Hou et al., 2021; Peng and Jimenez, 2021; Rudnick and Milton,

68   2003). In the literature, the derived thresholds were found to be highly sensitive to factors such

69   as activity level and community prevalence, making CO_2 thresholds varying across different

70   indoor spaces (Peng and Jimenez, 2021). For example, the reference excess CO_2 threshold

71   (above outdoor level) for classroom amounts to only about 150 ppm, while this figure is ten-

72   fold for supermarket (Peng and Jimenez, 2021). This indicates that the CO_2 thresholds should

73   be determined case by case, instead of setting a fixed value for all spaces.

74   In addition, most proposed thresholds are for spaces with fixed occupancy level under the

75   assumption of no initial quanta/excess CO_2 (Hou et al., 2021; Peng and Jimenez, 2021; Rudnick

76   and Milton, 2003). For spaces with variable occupancy, some of quanta/CO_2 released by the

77   previous group of occupants can remain in the space and become initial quanta/CO_2 when the

78   next group occupies the space, hence increasing the infection risk for the current occupants.

79   The initial quanta is essential for defining CO_2 threshold, but it is difficult to estimate as it

80   requires information of ventilation condition and occupancy profile of previous occupancy

81   stage. Hence, how to account for initial quanta/excess CO_2 in spaces with changing occupancy

82   in infection risk assessment remains an unsolved question (Mittal et al., 2020b; Wei and Li,

83   2016).

84   Finally, emissions of quanta and CO_2 are two important parameters in determining the CO_2

85   threshold, but they have inter-individual variation and can also be affected by factors such as

86   age and gender (Buonanno et al., 2020a; Persily and de Jonge, 2017; Good et al., 2021). For

87   instance, the viral load of super-spreader can be 10 times higher than the mean level of normal

88   infectious subjects (Lelieveld et al., 2020), which may indicate a higher quanta emission (Ke

89   et al., 2021, 2022). Different values of quanta and CO_2 emission were adopted by previous

90   studies for CO_2 threshold derivation, e.g., from 0.37 quanta/h to 100 quanta/h for classrooms

91   (Buonanno et al., 2020a; Bazant et al., 2021; Hou et al., 2021; Peng and Jimenez, 2021). The

92   effect on the uncertainty on the emissions of quanta and CO_2 on defining a CO_2 threshold

93   should be further analyzed. The present study aims to provide a new calculation framework to

94   derive safe excess CO_2 thresholds (C_t) by considering initial quanta/excess CO_2 and

95   changing/fixed occupancy patterns for different indoor spaces, as well as propagating the

96   uncertainty of these input variables.

97   **2. Methodology**

98 *2.1 General calculation framework*

99 Our model is based on four assumptions for indoor mass balance equations for CO_2 and

100 quanta (Hou et al., 2021): 1) both CO_2 and quanta are well mixed and evenly distributed in

101 the air; 2) indoor excess CO_2 is released by human exhalation only, with no other indoor

102 sources; 3) CO_2 emission rate and quanta emission rate are both constant (i.e., not time

103 dependent); 4) the loss of quanta is mainly due to ventilation, other elimination mechanisms

104 such as deposition, filtration and inactivation are neglected.

105 In deriving C_t for spaces with changing occupants, we consider a sequence of occupancy

106 stages, $S_i(I_i, N_i, T_i)$. Stage i represents an indoor space (with the volume of V) being occupied

107 by a number of occupants (N_i) with infectors (I_i) for a duration of time (T_i). $i =1$ represents the

108 start of the occupancy: N_1 occupants (with I_1 infectors) stay in this indoor space for a period of

109 T_1, with no people inside prior to N_1 occupants. The introduction of various occupancy stages

110 aims to consider the virus released and still in the air from previous occupancy stages (the

111 initial quanta). This is fundamentally different from previous studies which only considered

112 one-off occupancy or fixed occupancy throughout the exposure period of interest.

113 The general calculation process of C_t for one occupancy stage of a space is given as follows.

114 Long-range transmission risk for occupancy stage i is modeled through a Wells-Riley model

115 (Riley et al., 1978) amended by Gammitoni and Nucci (1997) to assess infection risk through

116 unsteady-state quanta concentration:

$$P_i = 1 - e^{-B \int_0^{T_i} C_{q,i}(t)dt} \tag{1}$$

118 Quanta concentration in Equation (1) is modeled through transient mass balance equation:

$$\frac{dC_{q,i}}{dt} = \frac{I_i E_q}{V} - \lambda_i C_{q,i} \tag{2}$$

120   Equation (2) can be analytically solved as:

121
$$C_{q,i}(t) = \left(C_{qin,i} - \frac{I_i E_q}{\lambda_i V} \right) e^{-\lambda_i t} + \frac{I_i E_q}{\lambda_i V} \tag{3}$$

122   To control transmission risk of stage i under an acceptable low level, a risk threshold of P_t

123   needs to be initially determined. Based on P_t, a required ACH (air change rate, λ_i) can be

124   derived by substituting Equation (3) into Equation (1), λ_i should be no less than the derived

125   value to keep transmission risk under P_t.

126   Indoor excess CO_2 concentration is also dominated by ACH, hence it reflects the ventilation

127   condition of stage i.

128   Indoor excess CO_2 concentration for stage i is determined by mass balance equation (4):

129
$$\frac{dC_{CO2,i}}{dt} = \frac{N_i E_{CO2}}{V} - \lambda_i C_{CO2,i} \tag{4}$$

130   Equation (4) is solved as:

131
$$C_{CO2,i}(t) = \left(C_{Cin,i} - \frac{N_i E_{CO2}}{\lambda_i V} \right) e^{-\lambda_i t} + \frac{N_i E_{CO2}}{\lambda_i V} \tag{5}$$

132   Substituting the required ACH that is backward calculated from transmission risk threshold

133   into Equation (5), the time-averaged indoor excess CO_2 concentration ($C_{CO2,i}$) during T_i is

134   exactly C_t for stage i (Hou et al., 2021; Bazant et al., 2021):

135
$$C_t = \frac{1}{T_i} \int_0^{T_i} C_{CO2,i}(t) dt \tag{6}$$

136   When indoor excess CO_2 concentration is below the reference threshold C_t, sufficient

137   ventilation can be promised to keep long-range transmission risk for occupancy stage i under

138   the risk level of P_t.

139   Further, for different occupancy stages, C_t can be derived by following the steps mentioned

140   above considering the existence of initial quanta/excess CO_2, see Equation (3) and Equation

141   (5). Starting from occupancy stage 1 without initial quanta/excess CO_2, a required ACH (λ_1)

142 can be easily obtained following the general calculation process. For occupancy stage 2, the

143 initial quanta and initial excess CO_2 can be estimated based on the ACH derived in occupancy

144 stage 1 (λ_1) under the assumption that excess CO_2 during occupancy stage 1 has been controlled

145 under the reference threshold, C_t for occupancy stage 2 can then be obtained according to the

146 calculation framework. Repeating these steps, i.e. by taking the derived ACH of previous

147 occupancy stage to estimate initial quanta/excess CO_2 for present stage, C_t can be calculated

148 iteratively for all the occupancy stages modeled.

149 *2.1.1 Infection Risk Threshold P_t*

150 The infection risk threshold P_t is of great importance as it dominates the safety levels of the

151 indoor environment. It can be defined in two ways, either by using a constant value for all

152 environment - such as 1%, 0.1% (Dai and Zhao, 2020) or even 0.01% (Peng and Jimenez -

153 2021) or to determine P_t based on reproductive number (R_A) where R_A is the average number

154 of secondary cases caused by one infector in a given susceptible population in indoor

155 environment. In the latter, the value of P_t is dominated by the number of occupants and can be

156 a large and inconvincible value when occupant number is small (Ma et al., 2018; Furuya et al.,

157 2009). In this study, we use a constant value of $P_t = 0.01\%$ as suggested in Peng and Jimenez

158 (2021), which is reasonable for most occupancy stages when the number of occupants is less

159 than 10,000.

160 *2.2 Designed Scenarios*

161 Three scenarios were identified to calculate C_t:

162   1) Regularly attended space with fixed occupancy level and the same group of people as

163   occupants, so that $N_1=N_2=...$ (e.g., a lecture room used by a certain group of students)

164   (Burridge et al., 2021; Vouriot et al., 2021) ;

165   2) Non-regularly attended space with constant infection ratio ($I_1/N_1=I_2/N_2=...=I_i/N_i$),

166   different groups of people as occupants, and with high occupancy level (e.g., shopping center,

167   train station);

168   3) Non-regularly attended space with changing infection ratio ($I_1/N_1 \neq I_2/N_2 \neq ... \neq I_i/N_i$) and low

169   occupancy level (e.g., gym, train coach).

170   All these scenarios are widely experienced in real-life situations.

171   *2.2.1 Scenario 1: Regularly attended spaces*

172   We determined the number of infectors I_i for Scenario 1 according to both the indoor

173   occupancy level (N_i) and local community prevalence (P_I). The expected I_i is defined as max

174     $\{1, P_I N_i\}$. When with a low indoor occupancy level or a low community prevalence, the value

175   of $P_I N_i$ can be less than 1, under such condition, I_i is assumed to be equal to 1, Otherwise, I_i is

176   assumed to be $P_I N_i$ to reflect the real local infection condition.

177   Derived from mass balance equations, quanta concentration and excess CO_2 concentration

178   were found to have a constant proportion during all the occupancy stages, only affected by

179   infection ratio and emissions, see Equation (7) (Full derivation details can be found in

180   Supplementary Information). As long as the infection ratio and emissions do not change during

181   the occupancy stages, the proportion remains unchanged as well, hence:

182
$$\frac{C_{q,1}(t)}{C_{CO2,1}(t)} = \frac{C_{q,2}(t)}{C_{CO2,2}(t)} = \cdots = \frac{I_i}{N_i}\frac{E_q}{E_{CO2}} \tag{7}$$

183   Under these circumstances, infection risk for stage i Eq (1) can be revised as below

184
$$P_i = 1 - e^{-B\frac{I_i}{N_i E_{CO2}}\frac{E_q}{\int_0^{T_i}} C_{CO2,i}(t)dt} \tag{8}$$

185   Equation (8) can be treated as the classical rebreathed fraction (RF) -based infection risk

186   model derived by Rudnick and Milton (2003), with $BC_{CO2,i}(t)/E_{CO2}$ representing the

187   rebreathed fraction. This derivation proved that rebreathed fraction (RF) -based model can

188   account for the impact of initial quanta/excess CO_2 in risk assessments for spaces with fixed

189   occupants.

190   Based on Equation (8), the time averaged value C_t for occupancy stage i can then be derived

191   as:

192
$$C_t = \frac{E_{CO2}N_i}{E_q T_i B I_i} ln\left(\frac{1}{1-P_t}\right) \tag{9}$$

2.2.2 Scenario 2: Non-regularly attended spaces with constant infection ratios

194   In Scenario 2, we assumed that community prevalence (P_I) can be directly used to represent

195   indoor infection ratio due to the high occupancy level ($I_1/N_1=I_2/N_2=...=P_I$). The proportion

196   between $C_{q,i}$ and excess $C_{CO2,i}$ also become constant due to the constant infection ratio among

197   occupancy stages (Detailed derivation process can be found in Supplementary Information):

198
$$\frac{C_{q,1}(t)}{C_{CO2,1}(t)} = \frac{C_{q,2}(t)}{C_{CO2,2}(t)} = \cdots = P_I\frac{E_q}{E_{CO2}} \tag{10}$$

199   Similar as Scenario 1, the infection risk and excess CO_2 threshold can then be derived as:

200
$$P_i = 1 - e^{-BP_I\frac{E_q}{E_{CO2}}\int_0^{T_i} C_{CO2}(t)dt} \tag{11}$$

201
$$C_t = \frac{E_{CO2}}{E_q T_i B P_I} ln\left(\frac{1}{1-P_t}\right) \tag{12}$$

202   Equation (11) can be treated as an extension of the classical RF-based infection risk model.

203   The generality of the original model is extended from scenarios with fixed occupants (scenario

10

204   1) to scenarios with varying occupancy levels (scenario 2), with initial quanta/excess CO_2 to

205   be taken into account. It should be noted that T_i in Scenario 2 is usually hard to monitor as the

206   occupancy level keeps changing. An alternative method is to predefine it according to the

207   characteristics of different spaces. For example, T_i could be set as 35 min for check-in hall and

208   100 min for departure hall according to the average dwelling times measured in an airport (Mihi

209   et al., 2018).

210   *2.2.3 Scenario 3: Non-regularly attended spaces with changing infection ratios*

211   In Scenario 3, indoor infection ratio cannot be represented by P_I due to the relatively low

212   occupancy level. I_i is therefore recommended as the maximum value of $\{1, N_i P_I\}$ to provide a

213   safe indoor environment (as Scenario 1). In these circumstances, the infection ratio would

214   change among the occupancy stages and quanta concentration, and it would not be represented

215   by excess CO_2 concentration: C_t derivation needs to follow the general calculation process (see

216   Part 2.1).

217   It should be noted that the general calculation process does not require the field measurement

218   of ACH but relies on a known occupancy profile including the number of occupants and the

219   duration of occupancy for all the occupancy stages. Thus, this method may be more suitable

220   for spaces in Scenario 3 where the occupancy profile of N_i and T_i of each occupancy stage can

221   be monitored simultaneously or obtained before the spaces being occupied such as the rail train

222   or theatre.

223   *2.3 Uncertainty analysis and inputs*

224   Uncertainty analysis was carried out considering E_q and E_{CO2} have interindividual variation

225 and can vary with gender, age, leading uncertainty to C_t. The probability density functions

226 (PDF) of E_q for three different activities are from recent research of Buonanno et al. (2020a),

227 where they found the quanta emission follows a log10-normal distribution, see Table 1. E_{CO2}

228 was also assumed to be lognormally distributed with a standard deviation equal to 20% of its

229 mean (Molina and Jones, 2021). The mean value for the distribution is calculated as the average

230 value of E_{CO2} of female and male individuals aged 30 to 40 years (the most frequent age cohort)

231 with a specific metabolic equivalent (Persily and de Jonge, 2017). The metabolic equivalent

232 for E_{CO2} is specified by different activity levels, specifically, 1.5 met for sedentary activity, 3

233 met for light activity, 9 met for heavy activity (Ainsworth et al., 2000). Latin Hypercube

234 sampling (LHS) (Fang et al. 2005) was used to generate a total of 30,000 samples from

235 emissions of quanta and CO_2 due to its advantage in reflecting the true underlying distribution

236 of inputs with a smaller sample size. Monte Carlo simulations (Sobol', 1994) were used to

237 propagate and quantify the uncertainty in predictions.

238 **Table 1. Inputs for Uncertainty Analysis. Distribution mean and standard deviation in brackets**

Activity	Quanta emission PDF (quanta/h)	CO_2 emission PDF (mL/s)
Sedentary - breathing	LN10 (-0.429, 0.720)	LN (5.05, 1.01)
Light activity - speaking	LN10 (0.698, 0.720)	LN (10.10, 2.02)
Heavy activity - breathing	LN10 (0.399, 0.720)	LN (34.20, 6.84)

239 Typical indoor environments were selected for each scenario based on factors such as

240 occupancy level, infection ratio etc. (Tables 2 and 3). Cases in Scenario 1 have a fixed but

241 different number of occupants considering that this is a dominant parameter in deriving C_t in

242 Scenario 1, see Equation (9). It should be noted that the case of lecture hall in Scenario 1 has 3

243 infectors due to its high occupancy level, whereas other cases have only 1 infector due to the

244 relatively low occupancy level. In Scenario 2 a shopping center was taken as case study with

245 variable levels of community prevalence, which were adopted from three different COVID-19

246 periods in the UK for 2020 (Pouwels et al., 2021) to represent relatively small (0.06%), median

247 (0.4%) and high (1%) community prevalence, among which the highest level of community

248 prevalence was adopted for Scenario 1 and Scenario 3. Two cases with low and changing

249 occupancy levels were selected for Scenario 3 (i.e., train coach and gym room). As regards

250 occupancy stages, only one stage was included for cases in Scenario 1 and Scenario 2 whereas

251 five occupancy stages were included for cases in Scenario 3 to take into account the variability

252 in C_t due to the impact of initial quanta/excess CO_2. Different categories of activities were

253 considered in the cases of the different scenarios. Cases in Scenario 1 are assumed to have

254 "sedentary activity - breathing" typical of people sitting or standing in office or classroom

255 environments. Cases in Scenario 2 are assumed to have "light activity - speaking", considering

256 that people are usually walking in the shopping center and talking to each other. For scenario

257 3, two activities are included to explore the effects of activity level on C_t derivation, specifically,

258 "sedentary activity – breathing" for the train coach and "moderate activity – breathing" for

259 gym. The breathing rates (B) corresponding to different physical activity level is adopted are

260 from previous research (*Adams*, 1993).

261 **Table 2. Inputs of uncertainty analysis for Scenario 1 and Scenario 2.**

Case	Volume (m³)	Infector number	Occupant number	Exposure time (h)	Community prevalence	Breathing rate (m³/h)
Scenario 1						
Classroom	231	1	30	1	1%	0.54
Lecture classroom	270	1	65	1	1%	0.54
Lecture hall	540	3	300	1	1%	0.54
Open-plan office	594	1	20	1	1%	0.54
Scenario 2						

Shopping center	2040	-	-	1	0.06%, 0.4%, 1%	1.38

262 **Table 3. Inputs of uncertainty analysis for Scenario 3**

Scenario 3	Stage 1	Stage 2	Stage 3	Stage 4	Stage 5
Train coach (300 m^3)					
Infector number	1	1	1	1	1
Occupant number	20	40	80	40	20
Exposure time (h)	1	1	1	1	1
Community prevalence	1%	1%	1%	1%	1%
Breathing rate (m^3/h)	0.54	0.54	0.54	0.54	0.54
Gym (600 m^3)					
Infector number	1	1	1	1	1
Occupant number	5	10	20	10	5
Exposure time (h)	1	1	1	1	1
Community prevalence	1%	1%	1%	1%	1%
Breathing rate (m^3/h)	3.30	3.30	3.30	3.30	3.30

263 **3. Results**

264 *3.1 Safety excess CO_2 threshold varies in different scenarios*

265   For Scenario 1, the number of occupants (N_i) is the dominant factor governing C_t that scales

266 with it (see Equation (9)). C_t for cases with different N_i in Scenario 1 (regularly attended spaces)

267 have substantial differences, see Figure 1(a). The highest C_{t50} (the median value of C_t) occurs

268 in lecture hall (890 ppm), followed by lecture classroom (580 ppm), classroom (270 ppm), the

269 lowest one is in office environment (180 ppm), although significant overlaps exist in the output

270 distributions (Figure 1(a)).

271   For Scenario 2, instead of N_i, C_t is dominated by community prevalence (P_I), as C_t is

272 inversely proportional to P_I (see Equation (12)). Three different values of P_I (i.e., 0.06%. 0.4%

273 and 1%) are adopted to derive C_t and the results are showed in Figure 1(b). The highest C_{t50} of

274 870 ppm refers to the lowest P_I of 0.06% and the lowest C_{t50} of 50 ppm to the highest P_I of 1%.

275   For Scenario 3, the changing infection ratios lead to different values of C_t for different

276   occupancy stages. For train coach, C_{t50} are approx. 180 ppm, 320 ppm, 650 ppm, 410 ppm and

277   200 ppm corresponding to infection ratios of 1/20, 1/40, 1/80, 1/40 and 1/20 for the five stages

278   in sequence, while they are 7 ppm, 15 ppm, 30 ppm, 15 ppm and 7 ppm for gym environment

279   corresponding to infection ratios of 1/5, 1/10, 1/20, 1/10 and 1/5. The changing infection ratios

280   can lead to different C_t values in different stages mainly because the existence of initial

281   quanta/excess CO_2. For instance, for Stage 2 and Stage 4 of train coach with the same occupant

282   number of 40, C_{t50} should be same if initial quanta/excess CO_2 is not considered, but in fact the

283   difference of C_{t50} between the two occupancy stages reaches approx. 80 ppm due to the impact

284   of initial quanta/excess CO_2.

285   In addition, the general cases in Scenario 3 also proves that activity level is another major

286   factor which can affect the derived thresholds, see Figure 1(c). C_t for gym with a high activity

287   level is much lower than that for train coach with a sedentary activity level due to relative high

288   activity level in gym environment (hence, high emission rate for quanta). This agrees with

289   previous studies (Chen et al., 2022; Jia et al., 2022) that there should be much higher restriction

290   in spaces with high activities such as gym to control airborne infection risk.

291   Apart from the substantially different C_t among different cases, large uncertainty of C_t was

292   also found in each case, spanning up to six orders of magnitude on a log scale (see Figure 1).

293   Figure 1 shows that cases with a large median value contain more uncertainty due to a more

294   right-shifted log-scaled distribution of C_t, indicating that C_t can be more affected by the

295   uncertainty of emission settings considered in our study. Considering the large uncertainty of

296   C_t and the non-normal distribution when transformed to a linear scale, the median safe excess

297   CO_2 threshold (C_{t50}) is an appropriate descriptive statistic for excess CO_2 threshold due to its

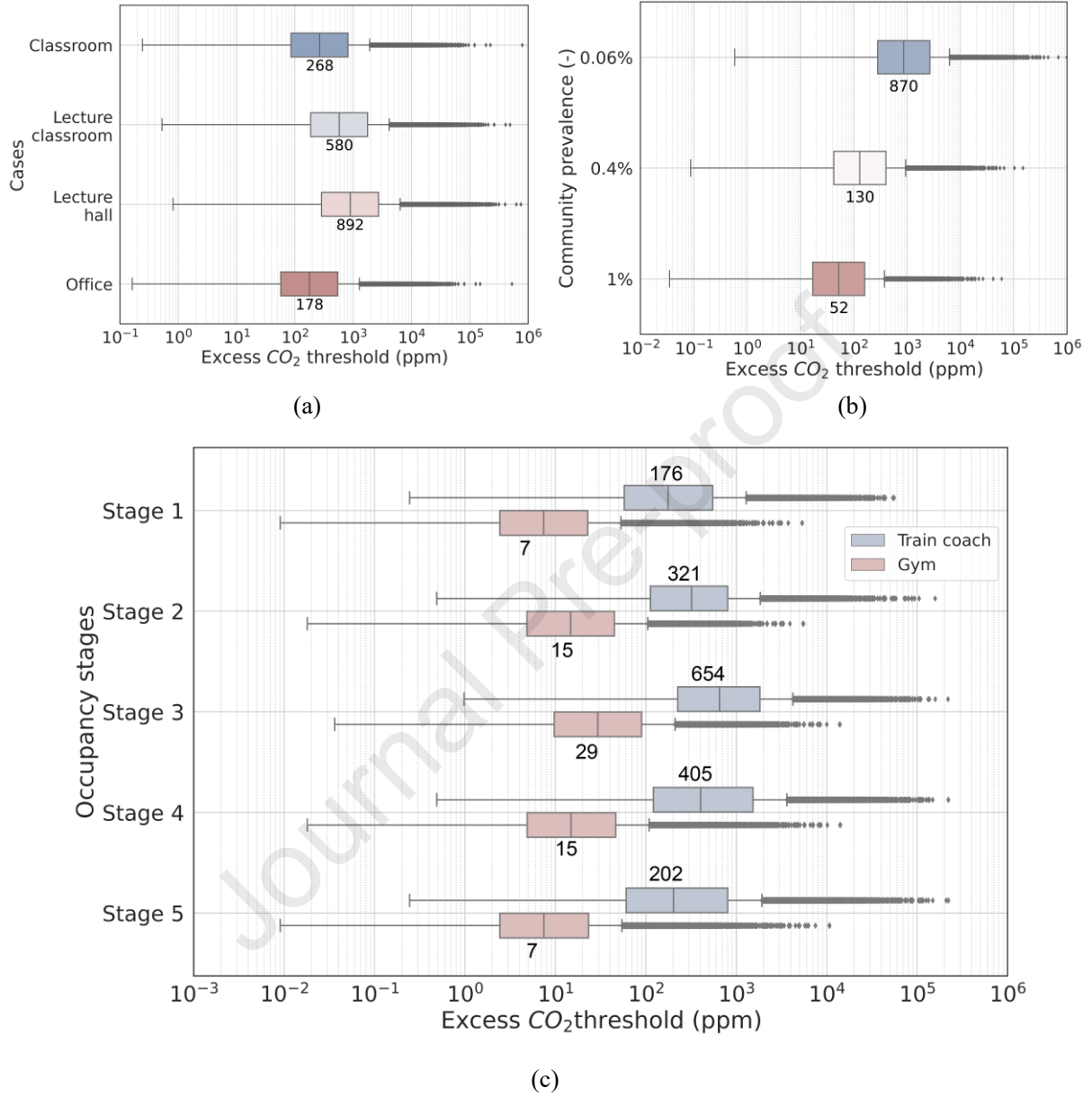298 high probability density (see the violin plot in Figure 1) (Jones et al., 2021).

299

(a)

(b)

300

301

302 (c)

303 **Figure 1.** Safe excess CO_2 thresholds for 3 scenarios: (a) Scenario 1(with fixed occupancy);

304 (b) Scenario 2 (with changing occupancy but fixed infection ratios); (c) Scenario 3 (with

305 changing occupancy and non-fixed infection ratios).

306 3.2 Effect of infection risk threshold (P_t)

307 As discussed before, the infection risk threshold (P_t) plays a role in deriving C_t. Different P_t

308 have been adopted in different research in the range of 0.01% to 1% (Buonanno et al., 2020b;

309 Dai and Zhao, 2020; Peng and Jimenez, 2021; Zhang et al., 2021). Here we explore how P_t will

310 affect C_t with results shown in Figure 2. The base case is the classroom in Scenario 1 (see Table

311 2). C_{t50} is found to be approximately linearly related to P_t with approx. 270 ppm for $P_t = 0.01\%$

312 to 27000 ppm for $P_t = 1\%$, which reveals the high sensitivity of C_{t50} to P_t.
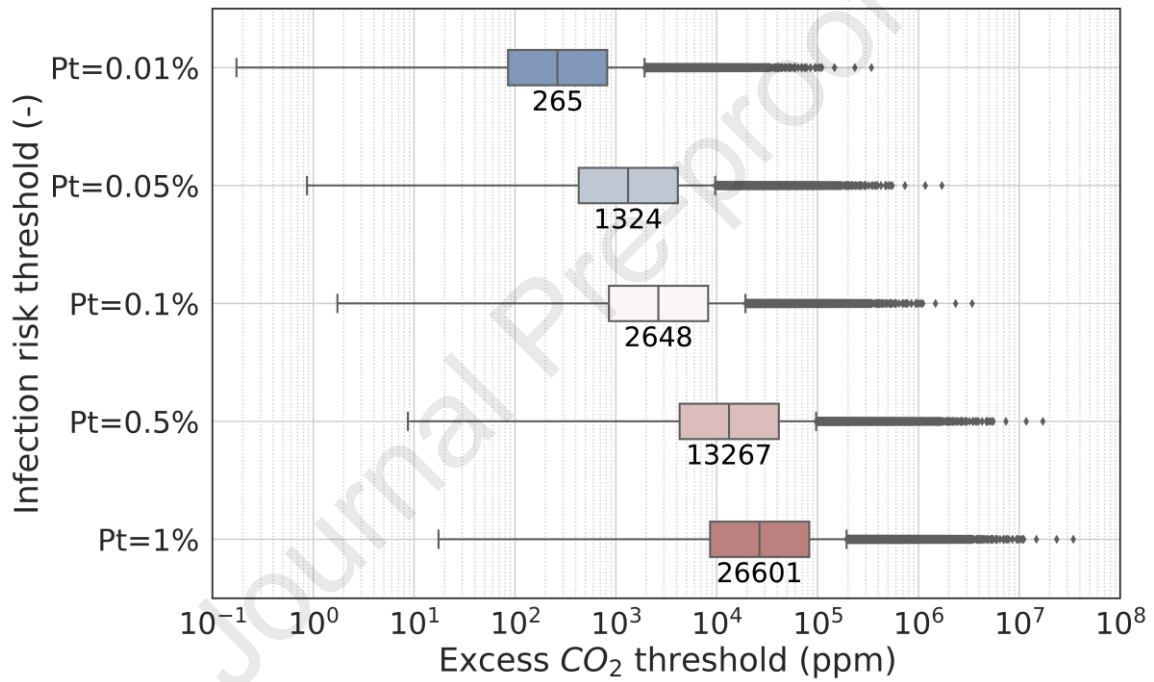
313

314 **Figure 2.** Excess CO_2 thresholds for the classroom (see Table 2) under different infection risk

315 thresholds.

316 *3.3 Effect of Initial Conditions*

317 We have shown that initial condition of quanta and excess CO_2 can affect the derived safe

318 excess CO_2 threshold when infection ratio varies among the occupancy stages. However, most

319 previous studies overlook the initial condition of quanta and excess CO_2 in C_t derivation (Hou

320 et al., 2021; Peng and Jimenez, 2021; Rudnick and Milton, 2003). To further quantify the

321   impact of initial condition of quanta/excess CO_2 on C_t when infection ratio varies, we compare

322   two cases: 1) considering the initial condition of quanta/excess CO_2; 2) no initial quanta/excess

323   CO_2. We consider two cases with the same indoor volume of 300 m^3, being occupied both with

324   two stages. The occupants in the two cases are assumed to have "sedentary activity – breathing",

325   and only 1 infector is adopted.

326   Case 1 assumes there are 20 occupants in Stage 1, and the occupant number in Stage 2

327   changes to 5, 10, 20, 40, 80 respectively, which means the infection ratio will change from 1/20

328   (Stage 1) to 1/5, 1/10, 1/20, 1/40, 1/80 (Stage 2) accordingly and initial quanta/excess CO_2 can

329   affect C_t in Stage 2 in varying degrees. Case 2 assumes there are no occupants in Stage 1 (hence

330   no initial quanta/excess CO_2), and 5 different occupancy levels are assumed for Stage 2 just

331   like case 1. Here we aim to derive C_t for Stage 2 for both two cases with consideration of the

332   impacts of initial quanta/excess CO_2 from Stage 1 (case 1) and without (case 2). The differences

333   of results between the two cases can be used to quantify the impact of initial quanta/excess CO_2

334   on C_t. It's easy to derive C_t for case 2 as there are no initial quanta/excess CO_2, while for case

335   1, an estimation of initial quanta/excess CO_2 released from stage 1 is needed. Considering the

336   excess CO_2 concentration is affected by different factors such as exposure time and ACH during

337   Stage 1, here we assumed a constant value for initial excess CO_2 concentration for Stage 2 in

338   case 1, namely, 1000 ppm. Initial quanta can then be derived based on it and infection ratios of

339   Stage 1 (see Eq. S4 in Supplementary).

340   Figure 3 shows there are distinct differences of derived C_t between the cases with and

341   without considering initial quanta/excess CO_2 when infection ratio of Stage 2 differs from

342   Stage 1 (1/20), suggesting the initial condition of quanta/excess CO_2 shouldn't be ignored in

343   C_t derivation. Overall, when infection ratio increases (larger than 1/20) from Stage 1, C_t

344   considering initial condition is larger than that without considering initial quanta/excess CO_2,

345   and vice versa. The difference will be higher when the infection ratio deviates more from the

346   base case of 1/20. When the infection ratio increases from 1/20 (Stage 1) to 1/5 (Stage 2), C_{t50}

347   increases by 60 ppm than that without considering initial quanta/excess CO_2 and when the

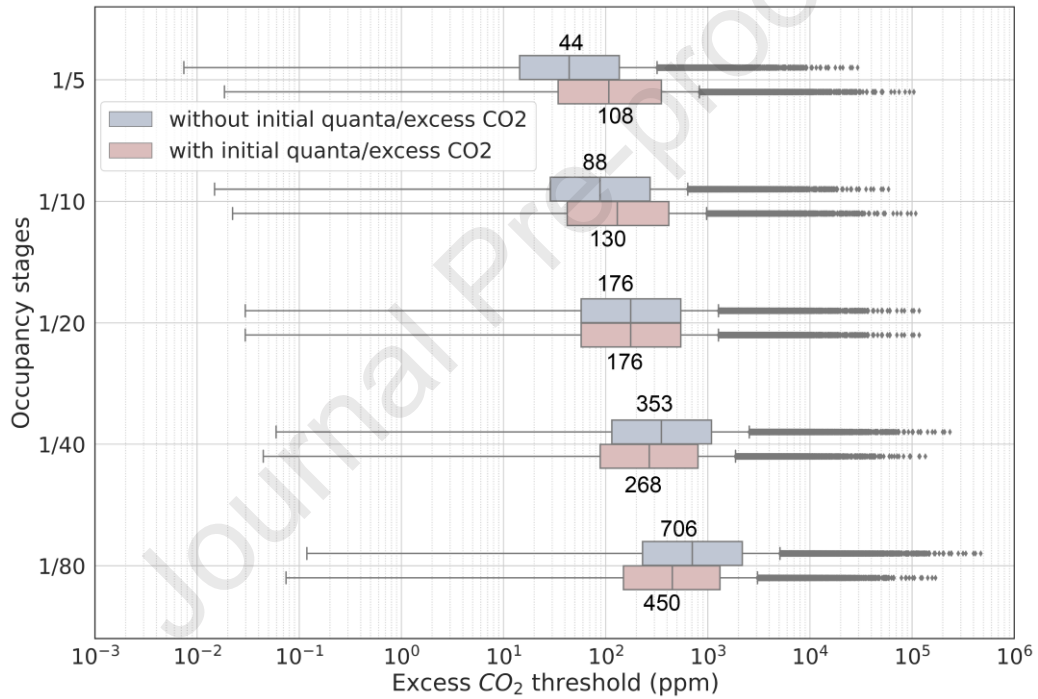348   Stage 2 infection ratio decreases from 1/20 to 1/80, C_{t50} becomes 260 ppm lower.

349

350   **Figure 3.** Excess CO_2 threshold of the second occupancy stage of an indoor space (300 m^3)

351   under different infection ratios considering with and without initial quanta/CO_2

352   **4. Discussion**

353   *4.1. New understanding of rebreathed-fraction model*

354   RF-based Wells-Riley model proposed by Rudnick and Milton's (2003) used CO_2 as a maker

355 for exhaled-breath exposure and avoided ACH estimation for airborne infection risk

356 assessment. The model does not require any knowledge about ACH, hence it has been widely

357 used in assessing airborne infection risk (Andrews et al., 2014; Hella et al., 2017; Richardson

358 et al., 2014; Wood et al., 2014; Zürcher et al., 2020). However, However, we proved that RF-

359 based model should be only adopted for spaces with fixed occupancy otherwise initial quanta

360 will cause bias of it (see Part 3.3), but this is largely overlooked by many other studies. For

361 spaces with varying occupancy, the initial quanta/excess CO_2 generated by previous occupants

362 but remaining in the air can be very important determining the overall quanta/excess CO_2

363 concentration for next-stage occupancy. How will RF-based model deal with initial

364 quanta/excess CO_2 for spaces with changing occupancy has not been adequately discussed

365 before. In this article, we made analytical derivation to explain the mechanism of RF-based

366 method in dealing with initial quanta/excess CO_2. We showed that initial quanta/excess CO_2

367 can be considered within the RF-based method in C_t derivation for Scenario 1 (with fixed

368 occupancy) and Scenario 2 (with changing occupancy but fixed infection ratios). This further

369 extends the generalization of RF-based model from spaces with fixed occupancy to spaces with

370 changing occupancy. It should be noted that other recent studies (Burridge et al., 2021; Vouriot

371 et al., 2021) resonate with our study in that they apply RF-based model to spaces with varying

372 occupancy levels to assess infection risk. However, only two occupancy modes were

373 considered in these studies, occupied and non-occupied, which are both included in our

374 Scenario 1. In this contribution, we have proved that for spaces with both occupied and non-

375 occupied modes, the non-occupied period does not affect the proportion of quanta

376 concentration to excess CO_2 concentration in future occupied period if infection ratios remain

377   unchanged given only ventilation is considered here (see Supplementary Information).

4.2. Implications for C_t determination

379   Great uncertainty in C_t can be caused by the uncertainty of emissions (E_q and E_{CO2}) (see

380   Figure 1). E_{CO2} and E_q contain uncertainty because they have interindividual variation and can

381   be affected by factors such as age, gender (Buonanno et al., 2020a; Persily and de Jonge, 2017;

382   Good et al., 2021). The value of E_q can vary by up to 3 orders of magnitude (e.g., 0.32-240

383   quanta/h for speaking under light activity) (Buonanno et al., 2020a) while E_{CO2} varies within

384   only one order of magnitude (e.g., 2.88-43.2 L/h) (Persily and de Jonge, 2017). Different

385   studies adopted very different values of E_q and therefore could lead to very different C_t. For

386   only the classroom settings with the same activity level, the median value of E_q in our study is

387   0.37 quanta/h (Buonanno et al., 2020a), while it was in the range of 27.55 quanta/h to 100

388   quanta/h in other studies (Bazant et al., 2021; Hou et al., 2021; Peng and Jimenez, 2021),

389   resulting in several hundred times lower C_t than our results.

390   The choice of P_t and I_i have also an impact C_t. Theoretically, lower P_t can promise safer

391   indoor environment, but this would come at the cost of very low C_t practically impossible to

392   achieve in real-world scenarios. E.g., a low level of C_t may require a very high ACH, unfeasible

393   and prone to cause large energy cost due to the diminishing return phenomenon of ventilation

394   (Li et al., 2021). Besides, how to determine the infector number I_i is also important as it is

395   related to the total quanta emission. Our study defined I_i to be the maximum value of $\{1, P_lN_i\}$

396   as the worst-case scenario. On the contrary, Bazant et al. (2021) considered I_i to be the

397   minimum value of $\{1, P_lN_i\}$, which resulted in a dramatically large C_t (even larger than 10000

398   ppm) when P_I is small.

4.3. Implications for infection risk monitoring and control

400   Our model has practical significance for indoor transmission monitoring and control. For

401   Scenario 1 and Scenario 2, safe excess CO_2 threshold is related to variables such as occupancy

402   level, duration and risk threshold through simple equations (see Equation (9) and Equation

403   (12)), making it possible to apply our model for infection risk monitoring in Scenario 1 and 2

404   for public individuals. For instance, when arriving at a space such as a shopping center (as our

405   Scenario 2), people can easily measure the indoor excess CO_2 level first through a portable

406   low-cost CO_2 sensor, then by replacing C_t in Equation (12) by the measured data, people can

407   roughly obtain a safe exposure duration for that shopping center based on their acceptable risk

408   threshold to guide how long they should stay in the shopping center. Furthermore, taking into

409   account the impact of initial quanta/excess CO_2 on risk estimation and C_t derivation, our model

410   can be adopted to further develop different ventilation control strategies such as CO_2-based

411   demand-controlled ventilation (Li and Cai, 2022) or intermittent ventilation strategy (Melikov

412   et al., 2020; Zhang et al., 2022) with an objective to reduce indoor transmission risk by treating

413   indoor excess CO_2 as a control variable.

414   Further applying our calculation framework into real-world scenarios, some insights can be

415   gained by comparing derived C_t with measurement data/standard limits. For Scenario 1, the

416   occupant numbers can largely affect C_t level, thus, it's warranted to concurrently consider CO_2

417   level and occupant level in transmission risk evaluation of an indoor environment. For example,

418   for classrooms in Scenario 1, the measured excess CO_2 level was found to be in the range of

22

419   300 - 2500 ppm (outdoor level of 420 ppm) dependent on the number of occupants (Bakó-Biró

420   et al., 2012; Vouriot et al., 2021; Persily et al., 2022). According to our framework, 300 ppm

421   can represent an unsafe environment if the occupant number is less than 33, and 2500 ppm can

422   still be a safe level if occupants is larger than 278. Therefore, C_t threshold should be used in

423   conjunction with occupant number. For scenario 2, community prevalence can dominate C_t and

424   can be used as a reference for lockdown policy implementation. It was found that the one-hour

425   average CO_2 level of 40% shopping mall in Hong Kong exceeded 1000 ppm (Li et al., 2001).

426   To keep infection risk no more than 0.01% for shopping malls, a community prevalence of less

427   than 0.09% is needed according to our calculation framework, otherwise, such places should

428   be locked down. For Scenario 3, taking a restaurant (~350 m^3) for example, considering two

429   occupancy stage (N_1 = 20 for Stage 1 and N_2 = 80 for Stage 2) (Shen et al., 2021), according to

430   ASHRAE 62.1 (ASHRAE, 2019), the maximum excess CO_2 limits (the steady-state excess

431   CO_2 concentration under the required ventilation rate) for the first two occupancy stages are

432   540 ppm (Stage 1) and 790 ppm (Stage 2) respectively. But C_t calculated from our framework

433   amounts to 180 ppm and 610 ppm, respectively. The difference indicates the target of infection

434   risk control should be integrated into present ventilation standards to promise both a high level

435   of IAQ and a low infection risk.

436   *4.4. Limitation of the study*

437   Our study is based on the assumption that outdoor ventilation is the only loss mechanism

438   for quanta in Scenario 1 and Scenario 2, which results in a constant proportion between quanta

439   concentration and excess CO_2 concentration, hence making RF-based model suitable for

440   deriving C_t for Scenario 1 and 2. However, surface deposition, filtration and virus deactivation

441   could significantly contribute to reduce quanta concentration (Blocken et al., 2021; Su et al.,

442   2021; van Doremalen et al., 2020). Neglecting these loss mechanisms may overestimate indoor

443   quanta concentration and result in a lower estimate of C_t than needed. However, the reliability

444   of the derived C_t for a safe indoor environment would not be affected.

445   The thresholds we derived are based on the assumption of a well-mixed room air. Thus, the

446   location of CO_2 sensors needs to be carefully selected to adequately reflect indoor CO_2

447   conditions (Mahyuddin and Awbi, 2010; Mahyuddin et al., 2014). Additionally, our results only

448   account for long-range airborne transmission neglecting the contribution of short-range

449   transmission (Chen et al., 2021; Gao et al., 2021; Li, 2021). Limiting to monitoring infection

450   risk based on C_t values may not be sufficient. Other intervention measures such as wearing

451   masks and social distancing should be jointly considered to control indoor airborne

452   transmission (Jarvis, 2020; Mittal et al., 2020a; Wagner et al., 2021).

453   Another limitation lies in the application of community prevalence (P_I) in our study. For

454   scenario 1 and scenario 3, P_I is used to determine the indoor infector number, which would

455   cause bias because 1) P_I might be smaller than the real value due to the asymptomatic

456   characteristic of SARS-CoV-2 (Lee et al., 2020; Pollock and Lancaster, 2020); and 2) positive

457   individuals may not be present at public spaces due to mandatory quarantine policy which

458   would lead to a lower indoor infection ratio than P_I. For scenario 2, simply using P_I to represent

459   the indoor infection ratio can lead to underestimate the real indoor infection ratio when the

460   number of occupants is small. Conducting field measurement to estimate the average

461   occupancy level (N_{ave}) and selecting the maximum value of $\{1, N_{ave}P_I\}$ could be an alternative

462   method for defining a convincible infection ratio for scenario 2. In addition, considering P_I is

463   changing during different time periods of pandemic, the indoor infection ratio would need to

464   be updated accordingly.

465   In addition, the uncertainty of C_t estimated by our study may be limited as we only

466   considered the uncertainty in emission settings (i.e., quanta emission rate, CO_2 emission rate)

467   in C_t derivation. Community prevalence P_I may contain uncertainty due to the reasons

468   mentioned above. The uncertainty of it may increase the uncertainty of C_t for Scenario 2 where

469   P_I is a dominating input in C_t derivation, but it may not obviously affect C_t for Scenario 1 and

470   3 because P_I is adopted in C_t derivation only when $P_I N_i > 1$ but the occupancy level (N_i) of

471   most cases in Scenario 1 and 3 is usually low and hence $P_I N_i < 1$. Similar as emission settings,

472   breathing rate can also contain uncertainty due to interindividual differences and factors such

473   as age and gender. In addition, quanta emission rate, CO_2 emission rate and breathing rate may

474   all be correlated to each other (Good et al., 2021). In our study, we simply adopted constant

475   breathing rates for different physical activity levels following the study of Buonanno et al.

476   (2020a) which estimated the quanta emission rate under different physical activity levels.

477   Quanta emission rate and CO_2 emission rate are also inter-related through physical activity

478   level (See Table 1). In future, based on more accurate data, the uncertainty and correlation of

479   those parameters may be further interpreted, and the uncertainty of C_t can be therefore further

480   estimated.

481   **5. Conclusion**

482   A new calculation framework was proposed in this study for deriving safe excess CO_2

483   threshold (C_t) for different spaces with consideration of initial quanta/excess CO_2 and

484   fixed/changing occupancy levels. From our derivation process we found that the proportion of

485   indoor excess CO_2 concentration to quanta concentration is constant for a constant infection

486   ratio (infectors/occupants) of an indoor space. Based on this relationship, RF-based (rebreathed

487   fraction-based) model can be directly applied for infection risk assessment and C_t derivation

488   when infection ratio is constant, but not applicable for the cases with varying infection ratios.

489   Affected by factors such as occupant number (N_i), community prevalence (P_I) and activity

490   level, the median value C_{t50} derived by our framework varies significantly among the selected

491   cases, with a minimum value of 7 ppm for gym to a maximum value of 890 ppm for lecture

492   hall, with long-tailed distributions. Initial quanta/excess CO_2 is found to largely affect C_t

493   especially when the infection ratio varies significantly among the occupancy stages. A bias of

494   several hundred ppm (e.g., 260 ppm for a space of 300 m^3 and with sedentary activity level)

495   could be made if the initial quanta in C_t derivation is not well considered. Our finding illustrates

496   that different CO_2 thresholds should be derived for different spaces and different occupancy

497   stages, rather than being fixed at a constant value for all spaces.

498   Large uncertainty was also found in derived thresholds for all cases, spanning approximately

499   6 orders of magnitude, which are mainly influenced by quanta emission rate (E_q) and CO_2

500   emission rate (E_{CO2}). For a better control of indoor infection risk through CO_2 monitoring, more

501   accurate input parameters would be needed.

502   **Acknowledgement**

References

506   Adams, W.C., 1993. Measurement of Breathing Rate and Volume in Routinely Performed Daily
507   Activities. Final Report. Human Performance Laboratory, Physical Education Department,
508   University of California, Davis. Human Performance Laboratory, Physical Education
509   Department, University of California, Davis. Prepared for the California Air Resources
510   Board, Contract No. A033-205, April 1993.

511   Ainsworth, B.E., Haskell, W.L., Whitt, M.C., Irwin, M.L., Swartz, A.M., Strath, S.J., O'Brien,
512   W.L., Bassett, J., Schmitz, K.H., Emplaincourt, P.O., Jacobs, J., Leon, A.S., 2000.
513   Compendium of physical activities: An update of activity codes and MET intensities. Med
514   Sci Sports Exerc 32. https://doi.org/10.1097/00005768-200009001-00009

515   Andrews, J.R., Morrow, C., Walensky, R.P., Wood, R., 2014. Integrating social contact and
516   environmental data in evaluating tuberculosis transmission in a South African township.
517   Journal of Infectious Diseases 210, 597–603. https://doi.org/10.1093/infdis/jiu138

518   ASHRAE, 2019. ANSI/ASHRAE Standard 62.1-2019, Ventilation for acceptable indoor
519   airquality. Peachtree Corners, GA: ASHRAE.

520   Bakó-Biró, Z., Clements-Croome, D.J., Kochhar, N., Awbi, H.B., Williams, M.J., 2012.
521   Ventilation rates in schools and pupils' performance. Build Environ 48, 215–223.
522   https://doi.org/10.1016/j.buildenv.2011.08.018

523   Bazant, M.Z., Kodio, O., Cohen, A.E., Khan, K., Gu, Z., Bush, J.W.M., 2021. Monitoring
524   carbon dioxide to quantify the risk of indoor airborne transmission of COVID-19. Flow 1,
525   1–17. https://doi.org/10.1017/flo.2021.10

526   Blocken, B., van Druenen, T., Ricci, A., Kang, L., van Hooff, T., Qin, P., Xia, L., Ruiz, C.A.,
527   Arts, J.H., Diepens, J.F.L., Maas, G.A., Gillmeier, S.G., Vos, S.B., Brombacher, A.C.,
528   2021. Ventilation and air cleaning to limit aerosol particle concentrations in a gym during
529   the   COVID-19   pandemic.   Building   and   Environment   193,   107659.
530   https://doi.org/10.1016/j.buildenv.2021.107659

531   Buonanno, G., Morawska, L., Stabile, L., 2020a. Quantitative assessment of the risk of airborne
532   transmission of SARS-CoV-2 infection : Prospective and retrospective applications.
533   Environ Int 145, 106112. https://doi.org/10.1016/j.envint.2020.106112

534   Buonanno, G., Stabile, L., Morawska, L., 2020b. Estimation of airborne viral emission : Quanta
535   emission rate of SARS-CoV-2 for infection risk assessment. Environ Int 141, 105794.
536   https://doi.org/10.1016/j.envint.2020.105794

537   Burridge, H.C., Fan, S., Jones, R.L., Noakes, C.J., Linden, P.F., 2021. Predictive and
538   retrospective modelling of airborne infection risk using monitored carbon dioxide. Indoor
539   and Built Environment 1420326X2110435. https://doi.org/10.1177/1420326x211043564

540   CDC, 2021. Ventilation in buildings. Atlanta: Centers for Disease Control and Prevention.
541   https://www.cdc.gov/coronavirus/2019-ncov/community/ventilation.html

542   Chen, N., Zhou, M., Dong, X., Qu, J., Gong, F., Han, Y., Qiu, Y., Wang, J., Liu, Y., Wei, Y., Xia,
543   J., Yu, T., Zhang, X., Zhang, L., 2020. Epidemiological and clinical characteristics of 99

544 cases of 2019 novel coronavirus pneumonia in Wuhan, China: a descriptive study. The
545 Lancet 395, 507–513. https://doi.org/10.1016/S0140-6736(20)30211-7

546 Chen, W., Qian, H., Zhang, N., Liu, F., Liu, L., Li, Y., 2022. Extended short-range airborne
547 transmission of respiratory infections. J Hazard Mater 422.
548 https://doi.org/10.1016/j.jhazmat.2021.126837

549 CIBSE, C., 2020. COVID-19 Ventilation Guidance. https://www.cibse.org/Coronavirus-
550 COVID-19

551 Dai, H., Zhao, B., 2020. Association of the infection probability of COVID-19 with ventilation
552 rates in confined spaces. Build Simul 13, 1321–1327. https://doi.org/10.1007/s12273-
553 020-0703-5

554 EMG/SPI-B, 2021. Application of CO2 monitoring as an approach to managing ventilation to
555 mitigate SARS-CoV-2 transmission. https://www.gov.uk/government/publications/emg-
556 and-spi-b-application-of-co2-monitoring-as-an-approach-to-managing-ventilation-to-
557 mitigate-sars-cov-2-transmission-27-may-2021

558 Fang, K.-T., Li, R., Sudjianto, A., 2005. Design and Modeling for Computer Experiments (1st
559 ed.). Chapman and Hall/CRC. https://doi.org/10.1201/9781420034899

560 Furuya, H., Nagamine, M., Watanabe, T., 2009. Use of a mathematical model to estimate
561 tuberculosis transmission risk in an Internet café. Environ Health Prev Med 14, 96–102.
562 https://doi.org/10.1007/s12199-008-0062-9

563 Gao, C.X., Li, Y., Wei, J., Cotton, S., Hamilton, M., Wang, L., Cowling, B.J., 2021. Multi-route
564 respiratory infection: When a transmission route may dominate. Science of the Total
565 Environment 752, 141856. https://doi.org/10.1016/j.scitotenv.2020.141856

566 Gammaitoni, L., Nucci, M. C., 1997. Using a mathematical model to evaluate the efficacy of
567 TB control measures. Emerging infectious diseases, 3(3), 335–342.
568 https://doi.org/10.3201/eid0303.970310

569 Good, N., Fedak, K.M., Goble, D., Keisling, A., L'Orange, C., Morton, E., Phillips, R., Tanner,
570 K., Volckens, J., 2021. Respiratory Aerosol Emissions from Vocalization: Age and Sex
571 Differences Are Explained by Volume and Exhaled CO2. Environ Sci Technol Lett 8,
572 1071–1076. https://doi.org/10.1021/acs.estlett.1c00760

573 Hella, J., Morrow, C., Mhimbira, F., Ginsberg, S., Chitnis, N., Gagneux, S., Mutayoba, B.,
574 Wood, R., Fenner, L., 2017. Tuberculosis transmission in public locations in Tanzania: A
575 novel approach to studying airborne disease transmission. Journal of Infection 75, 191–
576 197. https://doi.org/10.1016/j.jinf.2017.06.009

577 Hou, D., Katal, A., Wang, L. (Leon), Katal1, A., Wang, L. (Leon), 2021. Bayesian Calibration
578 of Using CO2 Sensors to Assess Ventilation Conditions and Associated COVID-19
579 Airborne Aerosol Transmission Risk in Schools. medRxiv 2021.01.29.21250791.

580 Jarvis, M.C., 2020. Aerosol Transmission of SARS-CoV-2: Physical Principles and
581 Implications. Front Public Health. https://doi.org/10.3389/fpubh.2020.590041

582 Jia, W., Wei, J., Cheng, P., Wang, Q., Li, Y., 2022. Exposure and respiratory infection risk via
583 the short-range airborne route. Build Environ 219.
584 https://doi.org/10.1016/j.buildenv.2022.109166

585 Jones, B., Sharpe, P., Iddon, C., Hathway, E.A., Noakes, C.J., Fitzgerald, S., 2021. Modelling
586 uncertainty in the relative risk of exposure to the SARS-CoV-2 virus by airborne aerosol
587 transmission in well mixed indoor air. Build Environ 191.

588   https://doi.org/10.1016/j.buildenv.2021.107617

589 Ke, R., Zitzmann, C., Ho, D. D., Ribeiro, R. M., and Perelson, A. S.: In vivo kinetics of SARS-
590   CoV-2 infection and its relationship with a person's infectiousness, Proc. Natl. Acad. Sci.

591   U. S. A., 118, https://doi.org/10.1073/pnas.2111477118, 2021.

592 Ke, R., Martinez, P. P., Smith, R. L., Gibson, L. L., Mirza, A., Conte, M., Gallagher, N., Luo,
593   C. H., Jarrett, J., Zhou, R., Conte, A., Liu, T., Farjo, M., Walden, K. K. O., Rendon, G.,
594   Fields, C. J., Wang, L., Fredrickson, R., Edmonson, D. C., Baughman, M. E., Chiu, K. K.,
595   Choi, H., Scardina, K. R., Bradley, S., Gloss, S. L., Reinhart, C., Yedetore, J., Quicksall,
596   J., Owens, A. N., Broach, J., Barton, B., Lazar, P., Heetderks, W. J., Robinson, M. L.,
597   Mostafa, H. H., Manabe, Y. C., Pekosz, A., McManus, D. D., and Brooke, C. B.: Daily
598   longitudinal sampling of SARS-CoV-2 infection reveals substantial heterogeneity in
599   infectiousness, Nat Microbiol, 7, 640-652, 2022.

600 Li, B., Cai, W., 2022. A novel CO_2-based demand-controlled ventilation strategy to limit the
601   spread of COVID-19 in the indoor environment. Build Environ 219.
602   https://doi.org/10.1016/j.buildenv.2022.109232

603 Lee, S., Kim, T., Lee, E., Lee, C., Kim, H., Rhee, H., Park, S.Y., Son, H.J., Yu, S., Park, J.W.,
604   Choo, E.J., Park, S., Loeb, M., Kim, T.H., 2020. Clinical Course and Molecular Viral
605   Shedding among Asymptomatic and Symptomatic Patients with SARS-CoV-2 Infection
606   in a Community Treatment Center in the Republic of Korea. JAMA Intern Med 180,
607   1447–1452. https://doi.org/10.1001/jamainternmed.2020.3862

608 Lelieveld, J., Helleis, F., Borrmann, S., Cheng, Y., Drewnick, F., Haug, G., Klimach, T., Sciare,
609   J., Su, H., Pöschl, U., 2020. Model calculations of aerosol transmission and infection risk
610   of covid-19 in indoor environments. Int J Environ Res Public Health 17, 1–18.
611   https://doi.org/10.3390/ijerph17218114

612 Li, W.M., Lee, S.C., Chan, L.Y., 2001. Indoor air quality at nine shopping malls in Hong Kong.
613   Science of The Total Environment 273, 27–40. https://doi.org/10.1016/S0048-
614   9697(00)00833-0

615 Li, Y., 2021. Basic routes of transmission of respiratory pathogens—A new proposal for
616   transmission categorization based on respiratory spray, inhalation, and touch. Indoor Air.
617   https://doi.org/10.1111/ina.12786

618 Li, Y., Cheng, P., Jia, W., 2021. Poor ventilation worsens short-range airborne transmission of
619   respiratory infection. Indoor Air. https://doi.org/10.1111/ina.12946

620 Ma, Y., Horsburgh, C.R., White, L.F., Jenkins, H.E., 2018. Quantifying TB transmission: A
621   systematic review of reproduction number and serial interval estimates for tuberculosis.
622   Epidemiol Infect 146, 1478–1494. https://doi.org/10.1017/S0950268818001760

623 Mahyuddin, N., Awbi, H., 2010. The spatial distribution of carbon dioxide in an environmental
624   test chamber. Build Environ 45, 1993–2001.
625   https://doi.org/10.1016/j.buildenv.2010.02.001

626 Mahyuddin, N., Awbi, H.B., Alshitawi, M., 2014. The spatial distribution of carbon dioxide in
627   rooms with particular application to classrooms. Indoor and Built Environment 23, 433–
628   448. https://doi.org/10.1177/1420326X13512142

629 Melikov, A.K., Ai, Z.T., Markov, D.G., 2020. Intermittent occupancy combined with
630   ventilation: An efficient strategy for the reduction of airborne transmission indoors.

Science of the Total Environment 744. https://doi.org/10.1016/j.scitotenv.2020.140908

Mihi, Mirela, Ani, I.-D., Mihi, M, Professor, F., Ani, I., Kursan Milaković, I., Professor, A., 2018. Time spent shopping and consumer clothing purchasing behaviour EKONOMSKI PREGLED.

Miller, S.L., Nazaroff, W.W., Jimenez, J.L., Boerstra, A., Buonanno, G., Dancer, S.J., Kurnitski, J., Marr, L.C., Morawska, L., Noakes, C., 2021. Transmission of SARS-CoV-2 by inhalation of respiratory aerosol in the Skagit Valley Chorale superspreading event. Indoor Air 31, 314–323. https://doi.org/10.1111/ina.12751

Mittal, R., Meneveau, C., Wu, W., 2020a. A mathematical framework for estimating risk of airborne transmission of COVID-19 with application to face mask use and social distancing. Physics of Fluids 32. https://doi.org/10.1063/5.0025476

Mittal, R., Ni, R., Seo, J.H., 2020b. The flow physics of COVID-19. J Fluid Mech 894. https://doi.org/10.1017/jfm.2020.330

Molina, C., Jones, B., 2021. Investigating Uncertainty in the Relationship between Indoor Steady-State CO_2 Concentrations and Ventilation Rates. Aivc. https://doi.org/10.13140/RG.2.2.16867.99361

Peng, Z., Jimenez, J.L., 2021. Exhaled CO_2 as a COVID-19 infection risk proxy for different indoor environments and activities. Environ Sci Technol Lett 8, 392–397. https://doi.org/10.1021/acs.estlett.1c00183

Peng, Z., Rojas, A. L. P., Kropff, E., Bahnfleth, W., Buonanno, G., Dancer, S. J., Kurnitski, J., Li, Y., Loomans, M. G. L. C., Marr, L. C., Morawska, L., Nazaroff, W., Noakes, C., Querol, X., Sekhar, C., Tellier, R., Greenhalgh, T., Bourouiba, L., Boerstra, A., Tang, J. W., Miller, S. L., and Jimenez, J. L.: Practical Indicators for Risk of Airborne Transmission in Shared Indoor Environments and Their Application to COVID-19 Outbreaks, Environ. Sci. Technol., 56, 1125-1137, 2022.

Persily, A., de Jonge, L., 2017. Carbon dioxide generation rates for building occupants. Indoor Air 27, 868–879. https://doi.org/10.1111/ina.12383

Persily, A., Bahnfleth, W., Kipen, H., Lau, J., Mandin, C., Sekhar, C., Wagocki, P. and Nguyen Weekes, L.,2022, ASHRAE's New Position Document on Indoor Carbon Dioxide,ASHRAE,Journal,
https://tsapps.nist.gov/publication/get_pdf.cfm?pub_id=934476

Riley, E. C., Murphy, G., Riley, R. L., 1978. Airborne spread of measles in a suburban elementary school. American journal of epidemiology, 107(5), 421–432. https://doi.org/10.1093/oxfordjournals.aje.a112560

Pollock, A.M., Lancaster, J., 2020. Asymptomatic transmission of covid-19. The BMJ. https://doi.org/10.1136/bmj.m4851

Pouwels, K.B., et al., 2021. Community prevalence of SARS-CoV-2 in England from April to November, 2020: results from the ONS Coronavirus Infection Survey. The Lancet Public Health 6, e30–e38. https://doi.org/10.1016/S2468-2667(20)30282-6

Qian, H., Miao, T., Liu, L., Zheng, X., Luo, D., Li, Y., 2021. Indoor transmission of SARS-CoV-2. Indoor Air 31, 639–645. https://doi.org/10.1111/ina.12766

Rudnick, S.N., Milton, D.K., 2003. Risk of indoor airborne infection transmission estimated from carbon dioxide concentration. Indoor Air 13, 237–245. https://doi.org/10.1034/j.1600-0668.2003.00189.x

675 REHVA, 2021. REHVA COVID-19 Guidance, version 4.1. Brussels, Belgium: Federation of
676 European Heating, Ventilation and Air Conditioning Associations.
677 https://www.rehva.eu/fileadmin/user_upload/REHVA_COVID-
678 19_guidance_document_V4.1_15042021.pdf

679 Richardson, E.T., Morrow, C.D., Kalil, D.B., Bekker, L.G., Wood, R., 2014. Shared air: A
680 renewed focus on ventilation for the prevention of tuberculosis transmission. PLoS One
681 9, 1–7. https://doi.org/10.1371/journal.pone.0096334

682 SAGE-EMG, 2020. EMG: Role of ventilation in controlling SARS-CoV-2 transmission.
683 https://www.gov.uk/government/publications/emg-role-of-ventilation-in-controllingsars-
684 cov-2-transmission-30-september-2020

685 Shen, J., Kong, M., Dong, B., Birnkrant, M.J., Zhang, J., 2021. A systematic approach to
686 estimating the effectiveness of multi-scale IAQ strategies for reducing the risk of airborne
687 infection of SARS-CoV-2. Build Environ 200.
688 https://doi.org/10.1016/j.buildenv.2021.107926

689 Sobol', I.M., 1994. A Primer for the Monte Carlo Method (1st ed.). CRC Press.
690 https://doi.org/10.1201/9781315136448

691 Su, A., Grist, S.M., Geldert, A., Gopal, A., Herr, A.E., 2021. Quantitative UV-C dose validation
692 with photochromic indicators for informed N95 emergency decontamination. PLoS ONE
693 16, 1–24. https://doi.org/10.1371/journal.pone.0243554

694 van Doremalen, N., Bushmaker, T., Morris, D.H., Holbrook, M.G., Gamble, A., Williamson,
695 B.N., Tamin, A., Harcourt, J.L., Thornburg, N.J., Gerber, S.I., Lloyd-Smith, J.O., de Wit,
696 E., Munster, V.J., 2020. Aerosol and Surface Stability of SARS-CoV-2 as Compared with
697 SARS-CoV-1. New England Journal of Medicine 382, 1564–1567.
698 https://doi.org/10.1056/nejmc2004973

699 Vouriot, C.V.M., Burridge, H.C., Noakes, C.J., Linden, P.F., 2021. Seasonal variation in
700 airborne infection risk in schools due to changes in ventilation inferred from monitored
701 carbon dioxide. Indoor Air 31, 1154–1163. https://doi.org/10.1111/ina.12818

702 Wagner, J., Sparks, T.L., Miller, S., Chen, W., Macher, J.M., Waldman, J.M., 2021. Modeling
703 the impacts of physical distancing and other exposure determinants on aerosol
704 transmission. J Occup Environ Hyg 1–15.
705 https://doi.org/10.1080/15459624.2021.1963445

706 Wei, J., Li, Y., 2016. Airborne spread of infectious agents in the indoor environment. Am J
707 Infect Control 44, S102–S108. https://doi.org/10.1016/j.ajic.2016.06.003

708 Wood, R., Morrow, C., Ginsberg, S., Piccoli, E., Kalil, D., Sassi, A., Walensky, R.P., Andrews,
709 J.R., 2014. Quantification of shared air: A Social and environmental determinant of
710 airborne disease transmission. PLoS One 9, 1–8.
711 https://doi.org/10.1371/journal.pone.0106622

712 Zhang, S., Ai, Z., Lin, Z., 2021. Occupancy-aided ventilation for both airborne infection risk
713 control and work productivity. Build Environ 188.
714 https://doi.org/10.1016/j.buildenv.2020.107506

715 Zhang, S., Niu, D., Lin, Z., 2022. Occupancy-aided ventilation for airborne infection risk
716 control: Continuously or intermittently reduced occupancies? Build Simul.
717 https://doi.org/10.1007/s12273-022-0951-7

718 Zürcher, K., Morrow, C., Riou, J., Ballif, M., Koch, A.S., Bertschinger, S., Liu, X., Sharma,

719   M., Middelkoop, K., Warner, D., Wood, R., Egger, M., Fenner, L., 2020. Novel approach
720   to estimate tuberculosis transmission in primary care clinics in sub-Saharan Africa:
721   Protocol of a prospective study. BMJ Open 10. https://doi.org/10.1136/bmjopen-2019-
722   036214

723

724 **Supplementary Information**

725 **Derivation Process for Scenario 1 and Scenario 2**

726   Scenario 1 and Scenario 2 have constant infection ratios among different occupancy stages, specifically,

727 $I_1/N_1 = I_2/N_2 = ... = I_i/N_i$.

728   For S_1 (the start occupancy stage) with no initial quanta and initial excess CO_2, the solved quanta

729 concentration ($C_{q,1}$) and excess CO_2 concentration ($C_{CO2,1}$) over time T_1 through mass balance equations can

730 be expressed as:

$$C_{q,1}(t) = -\frac{I_1 E_q}{\lambda_1 V}e^{-\lambda_1 t} + \frac{I_1 E_q}{\lambda_1 V} \tag{S1}$$

$$C_{CO2,1}(t) = -\frac{N_1 E_{CO2}}{\lambda_1 V}e^{-\lambda_1 t} + \frac{N_1 E_{CO2}}{\lambda_1 V} \tag{S2}$$

733   A fixed proportion between quanta and excess CO_2 during stage S_1 can be derived:

$$\frac{C_{q,1}(t)}{C_{CO2,1}(t)} = \frac{I_1}{N_1}\frac{E_q}{E_{CO2}} \tag{S3}$$

735   Because initial quanta concentration ($C_{qin,2}$) and initial excess CO_2 concentration ($C_{cin,2}$) for next

736 occupancy stage S_2 are exactly the concentrations at the end of S_1, thus, they also have the fixed proportion

737 relationship as:

$$\frac{C_{qin,2}(t)}{C_{Cin,2}(t)} = \frac{I_1}{N_1}\frac{E_q}{E_{CO2}} \tag{S4}$$

739   For S_2 (second occupancy stage), replacing initial quanta concentration ($C_{qin,2}$) by initial excess CO_2

740 concentration ($C_{Cin,2}$) on basis of the fixed proportion above and a constant infection ratio of $I_1/N_1 = I_2/N_2$,

741 quanta concentration and excess CO_2 concentration over time (T_2) can be expressed as:

$$C_{q,2}(t) = \frac{I_2}{N_2}\frac{E_q}{E_{CO2}}\left(\left(C_{Cin,2} - \frac{N_2 E_{CO2}}{\lambda_2 V}\right)e^{-\lambda_2 t} + \frac{N_2 E_{CO2}}{\lambda_2 V}\right) \tag{S5}$$

$$C_{CO2,2}(t) = \left(\left(C_{Cin,2} - \frac{N_2 E_{CO2}}{\lambda_2 V}\right)e^{-\lambda_2 t} + \frac{N_2 E_{CO2}}{\lambda_2 V}\right) \tag{S6}$$

744   A same proportion between quanta and excess CO_2 concentration can be found during occupancy stage

745 S_2:

$$\frac{C_{q,2}(t)}{C_{CO2,2}(t)} = \frac{I_2}{N_2}\frac{E_q}{E_{CO2}} \tag{S7}$$

747   If there exists a stage S_0 following stage S_2 that without occupancy (no occupants indoor during period

748 T_0), quanta and excess CO_2 remained by stage S_2 also experience a synchronously damping in fixed

749 proportion as S_2:

$$C_{q,0}(t) = \frac{I_2}{N_2}\frac{E_q}{E_{co2}}\left(C_{Cin,0}e^{-\lambda_0 t}\right) \tag{S8}$$

$$C_{CO2,0}(t) = C_{Cin,0}e^{-\lambda_0 t} \tag{S9}$$

$$\frac{C_{q,0}(t)}{C_{CO2,0}(t)} = \frac{I_2}{N_2}\frac{E_q}{E_{CO2}} \tag{S10}$$

753   Based on constant infection ratios ($I_1/N_1 = I_2/N_2 = ... = I_i/N_i$), a general analytical expression for quanta

754 concentration and excess CO_2 concentration for stage S_i can be concluded from the derivation process above:

755
$$C_{q,i}(t) = \frac{I_i}{N_i}\frac{E_q}{E_{CO2}}\left(\left(C_{\text{Cin,i}} - \frac{N_i E_{CO2}}{\lambda_i V}\right)e^{-\lambda_i t} + \frac{N_i E_{CO2}}{\lambda_i V}\right) \tag{S11}$$

756
$$C_{CO2,i}(t) = \left(C_{\text{Cin,i}} - \frac{N_i E_{CO2}}{\lambda_i V}\right)e^{-\lambda_i t} + \frac{N_i E_{CO2}}{\lambda_i V} \tag{S12}$$

757 For all occupancy stages in Scenario 1 and Scenario 2, quanta concentration and excess CO_2 concentration
758 possess a fixed proportion dominated by three parameters: (1) constant infection ratio; (2) constant quanta
759 emission rate; (2) constant CO_2 emission rate.

760
$$\frac{C_{q,i}(t)}{C_{CO2,i}(t)} = \frac{I_i}{N_i}\frac{E_q}{E_{CO2}} \tag{S13}$$

761 Replacing quanta concentration by excess CO_2 concentration, airborne infection risk for stage i can be
762 quantified through Wells-Riley equation based on the excess CO_2 concentration:

763
$$P = 1 - e^{-B\frac{I_i}{N_i}\frac{E_q}{E_{CO2}}\int_0^{T_i} C_{CO2,i}(t)dt} \tag{S14}$$

764 Equation (S14) can be converted directly into the classical rebreathed fraction-based infection risk model
765 (Rudnick and Milton, 2003) with $BC_{co2}(t)/E_{co2}$ representing the rebreathed fraction. Safe excess CO_2
766 threshold for occupancy stage S_i for Scenario 1 and Scenario 2 ($I_i/N_i = P_I$) can then be derived on basis of
767 Equation (S14) with a predefined risk threshold P_t:

768
$$C_t = \frac{E_{co2} N_i}{E_q T_i B I_i} ln\left(\frac{1}{1-P_t}\right) \tag{S15}$$

769 For each occupancy stage, the initial quanta released by previous stages has been considered in the
770 derivation of safe excess CO_2 threshold in Equation (S15). The application of the derived CO_2 threshold can
771 be extended to more general occupancy stages without limitation of no initial quanta in space.
772

773 **Reference**

774 Rudnick, S.N., Milton, D.K., 2003. Risk of indoor airborne infection transmission estimated from carbon
775   dioxide concentration. Indoor Air 13, 237–245. https://doi.org/10.1034/j.1600-0668.2003.00189.x
776
777
778
779
780
781
782
783

Highlights

- Rebreathed fraction-based model can be applied for spaces with changing occupants but constant infection ratios.
- Initial quanta and excess CO_2 lead to bias of determining excess CO_2 threshold when infection ratio changes.
- Excess CO_2 threshold contains large uncertainty and should be determined on a case-by-case basis.

Declaration of interests

☐ The authors declare that they have no known competing financial interests or personal relationships that could have appeared to influence the work reported in this paper.

☒ The authors declare the following financial interests/personal relationships which may be considered as potential competing interests:

Xiaowei Lyu reports financial support was provided by China Scholarship Council.